



ELSEVIER

Available online at www.sciencedirect.com

SCIENCE @ DIRECT®

Journal of Luminescence 105 (2003) 89–96

JOURNAL OF
LUMINESCENCEwww.elsevier.com/locate/jlumin

Photoluminescence characteristics of Pr^{3+} in ThO_2 : interplay of defects in a photo-induced charge transfer

S.V. Godbole^{a,b,*}, A.R. Dhobale^a, M.D. Sastry^a, Chung-Hsin Lu^b, A.G. Page^a^a Radiochemistry Division, Bhabha Atomic Research Center, Trombay, Mumbai 400 085, India^b Department of Chemical Engineering, Electronic and Electro-optical Ceramics Laboratory, National Taiwan University, Taipei, Taiwan, ROC

Received 21 October 2002; received in revised form 8 April 2003; accepted 13 May 2003

Abstract

Photo-luminescence studies of Pr^{3+} activated thorium oxide phosphor have revealed that mainly ${}^3\text{P} \rightarrow {}^3\text{H}_4$ and ${}^1\text{D}_2 \rightarrow {}^3\text{H}_4$ transitions with life-time of 30 and 600 μs are observed in this sample. An exponential reduction in the emission intensity of Pr^{3+} ions was observed on following continuous excitation with 275 nm corresponding to the f–d transition band of Pr^{3+} ions. Such a reduction in emission intensity was observed at all temperatures investigated in the range 90–330 K. The emission intensity recovered partially on dark storage only above 180 K. The recovery of emission intensity was also observed on the illumination of pre-exposed sample to light in the wavelength region 300–430 nm. Following illumination with 275 nm, Pr^{3+} activated thorium oxide phosphor has displayed a weak thermally stimulated luminescence. These results thus suggest that the optical excitation dynamically changes the state of the system under observation, and that changes are occurring in the valence state of Pr ions due to e/h transfer process on 275-nm exposure. On dark storage and also on 365-nm illumination of the pre-exposed sample, e/h traps recombine to cause emission signal recovery. The analysis of data on reduction in intensity obtained with exposure to 275 nm suggests the likelihood of the of Pr^{3+} ions existing at three different sites. The activation energies associated with the release of electrons from excited Pr^{3+} ions at different sites were determined from the temperature dependence of the photo-induced charge transfer process.

© 2003 Elsevier B.V. All rights reserved.

PACS: 61.80.Ba; 61.72.Cc

Keywords: Photoluminescence; Photoionization; Photo-induced charge transfer; $\text{ThO}_2\text{:Pr}^{3+}$; Pr^{3+}

1. Introduction

The optical properties of insulators doped with rare earth ions or transition elements are deter-

mined by the intra-ion transitions of the dopant ion [1]. The spectroscopic investigation of such materials is interesting because of their potential for applications as laser materials, scintillators, lamp phosphors, display devices, radiation dosimetry materials, etc. In many of these applications, the location of impurity ion states, relative to host valence and conduction band are important.

*Corresponding author. Tel.: +886-2363-5230; fax: +886-2362-3040.

E-mail address: shvagod@yahoo.co.in (S.V. Godbole).

Photoconductivity measurements, wavelength specific excitation of thermally stimulated luminescence (TSL) and photoelectron paramagnetic resonance (EPR) investigations are regularly utilized to understand the same [2–8]. In the present work, based on photoluminescence (PL) investigations of $\text{ThO}_2:\text{Pr}^{3+}$ system, it is shown that the activation energies involved in the electron transfer process can be determined by investigating changes in emission intensity on excitation with f–d band as a function of time and at different temperatures.

2. Experimental

$\text{ThO}_2:\text{Pr}^{3+}$ was prepared by mixing thorium nitrate and praseodymium nitrate in solution form. Pr was added to produce 1% Pr by weight in thorium oxide. The mixed solution was then dried under infrared heating, and the dry nitrate powder was heated at 600°C for 3 h in the furnace. The formation of thorium oxide was confirmed by recording the XRD pattern. The resulting $\text{ThO}_2:\text{Pr}^{3+}$ was palletized without any additive, for further investigations. PL studies were conducted using Edinburgh FL-900 lifetime fluorescence spectrometer with pulsed H_2 lamp as excitation source and using Hitachi F-2000 fluorescence spectrometer with 150 W Xe lamp as continuum source. The indigenously developed LNT cryostat for solid samples along with temperature controller working in the temperature range 80–350 K was used. The sample was mounted on the cold finger of the cryostat and the cryostat was placed in a Hitachi spectrometer to enable recording of excitation/emission spectra and also time-dependent intensity changes at fixed excitation and emission wavelengths.

3. Results and discussion

Rare earths in ThO_2 lattice substitute for tetravalent cations in the +3 charge state. Charge compensation can be achieved by various methods involving oxygen vacancies leading to different local site symmetries at the lanthanide site. PL and

TSL studies on Pr^{3+} activated thorium oxide have been reported by Bryesse et al. [9] and Harvey and Hallett [10]. Particularly, Harvey et al. have investigated UV-induced TSL in the system, while, Brassey et al. have mentioned the occurrence of at least two types of sites for Pr^{3+} ions in the matrix based on their investigations of PL intensity variation as a function of calcination temperature. Current investigations involve the measurement of PL characteristics of $\text{ThO}_2:\text{Pr}^{3+}$, including fluorescence lifetimes and observations regarding UV-induced changes in the intensity of fluorescence of Pr^{3+} ions at different temperatures in the temperature range 90–330 K.

3.1. Luminescence characteristics of $\text{ThO}_2:\text{Pr}^{3+}$ phosphor

Fig. 1 displays typical excitation spectra obtained for 500 nm emission from the sample at room temperature. The figure clearly reveals two excitation peaks, at 210 and 275 nm. The emission spectra recorded with 210 and 275 nm excitations are shown in Fig. 2. As presented in the figure, excitation with 210 nm basically causes emissions around 500 nm with weak emission around 620 nm, while, excitation with 275 nm shows strong 620 nm emission along with weak emission around 500 nm and weaker emission peaks at 590,

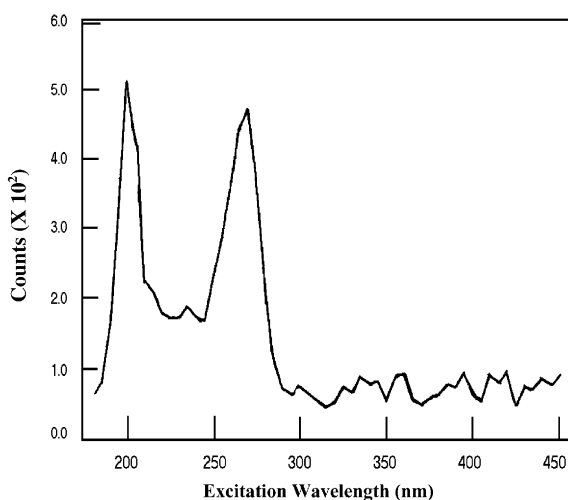


Fig. 1. Excitation spectra for $\text{ThO}_2:\text{Pr}^{3+}$ sample for 500 nm emission.

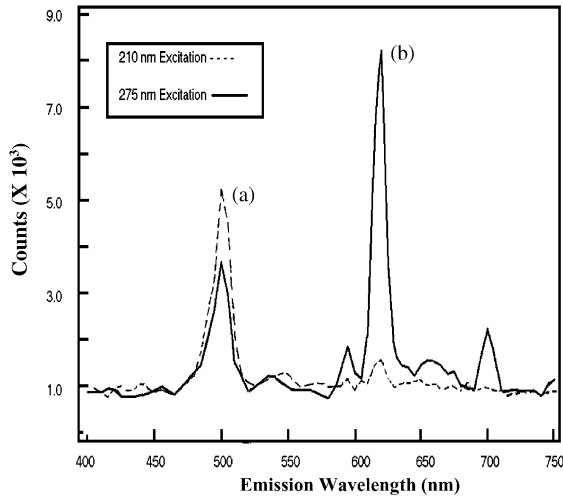


Fig. 2. Emission spectra for $\text{ThO}_2:\text{Pr}^{3+}$ sample on excitation with (a) 210 nm and (b) 275 nm.

655 and 700 nm. The lifetimes measured for 620 and 500 nm on excitation with 275 nm are 600 and 28 μs , respectively, at 300 K. The typical decay curves obtained for the two emission groups are shown in Figs. 3 and 4, respectively. The emission groups can be easily identified as due to $^1\text{D}_2 \rightarrow ^3\text{H}_4$ (620 nm), $^3\text{P} \rightarrow ^3\text{H}_4$ (500 nm) and their lifetimes are in the range reported for these transitions in variety of matrices [11]. Rodin and Land [12] have reported the bandgap for ThO_2 single crystal to be around 210 nm. The observed variation in relative intensities of 620 and 500 nm emission bands on excitation with 210 and 275 nm resembles that reported for two calcium zirconate in different phases [13]. Notably, these investigations have revealed that the nature of the emission depends on the position of the energy level corresponding to f^1d^1 electronic configuration of Pr^{3+} ions. In the case of lower energy position for f^1d^1 electronic configuration, the emission due to $^3\text{P}_{0,1} \rightarrow ^3\text{H}_4$ and $^1\text{D}_2 \rightarrow ^3\text{H}_4$ transitions are observed, while, in the case of higher energy position for the same, emission due to $^3\text{P}_{0,1}$ level are reported to be predominant. Consequently, excitation at 210 nm with a higher level position leads to prominent emission at 500 nm ($^3\text{P}_{0,1} \rightarrow ^3\text{H}_4$), while, excitation at 275 nm leads to observation of emission bands at 500 and 620 nm corresponding to $^3\text{P}_{0,1}$, $^1\text{D}_2 \rightarrow ^3\text{H}_4$ transition.

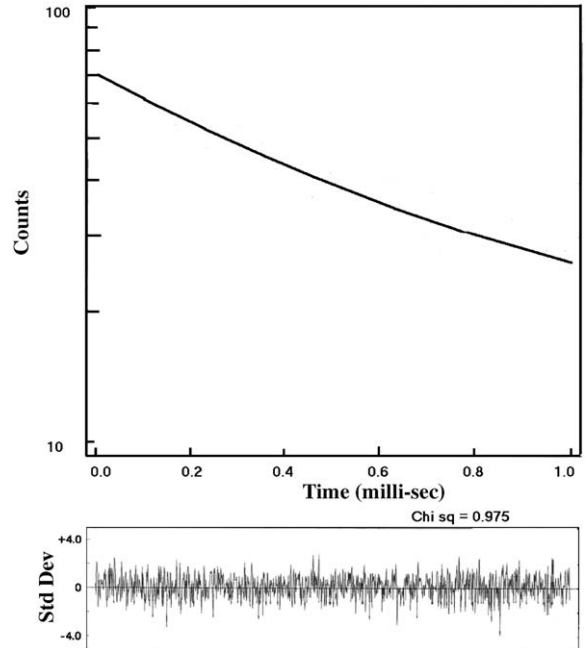


Fig. 3. Decay curve for 620 nm emission.

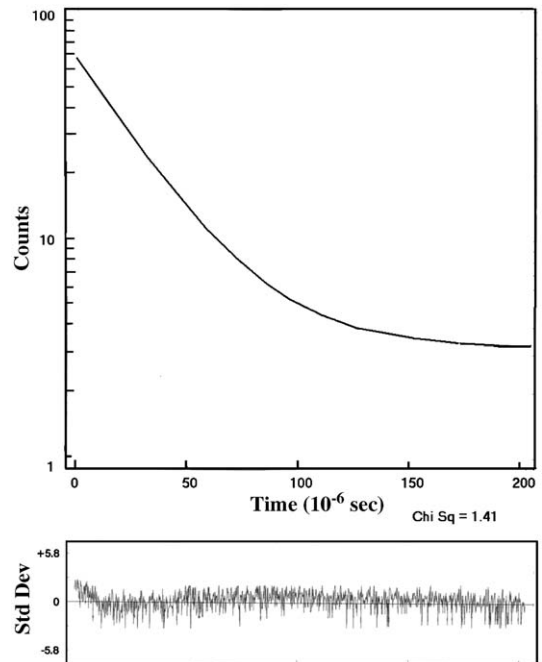


Fig. 4. Decay curve for 500 nm emission.

3.2. Photo-induced charge transfer processes

In subsequent studies Pr^{3+} intensity was monitored using 275-nm excitation and 500 nm emission on a Hitachi spectrometer under stable and continuous excitation. These investigations led to observation of changes in emission intensity on continuous excitation with an f–d band. To understand the dynamic process occurring on illumination with 275 nm, the emission intensity data was obtained as a function of illumination time at different temperatures. These investigations were carried out at a few select temperatures in the temperature range 90–330 K using indigenously developed LNT cryostat for solid samples along with temperature controller.

On continuous and extended illumination with 275 nm at all temperatures investigated, a decrease in emission intensity was observed. The typical observations at 270 K are shown in Fig. 5. The Fig. 5A shows the fall in intensity observed for virgin sample over a period of 100 s with exposure to 275-nm f–d band. The fall in intensity was observed to occur at all temperatures in the temperature range 90–330 K and suggests that Pr^{3+} ions are undergoing changes in concentration. Earlier investigations on $\text{CaF}_2:\text{Tb}^{3+}$ sample have revealed that a steady and stable luminescence is observed with the sample on exposure to 254 nm corresponding to f–d band of Tb^{3+} ions [14]. Using $\text{CaF}_2:\text{Tb}^{3+}$ sample to observe steady and stable emission intensity, it was confirmed that

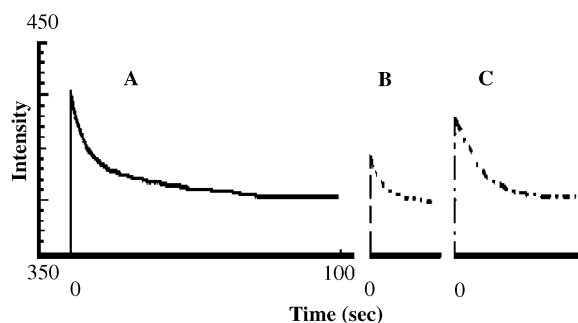


Fig. 5. Intensity variation observed with time on excitation with 275 nm and monitored with 500 nm emission at 270 K: (A) virgin sample, (B) pre-exposed sample A after 5 min of dark storage and (C) pre-exposed sample B after 5 min of exposure to 365 nm light from Xe lamp.

the present observation of reduction in emission intensity for $\text{ThO}_2:\text{Pr}^{3+}$ sample was not due to instrumental characteristic. For $\text{ThO}_2:\text{Pr}^{3+}$ pre-exposed sample, the intensity was monitored after storage in the dark lasting 5 min and the intensity changes are shown in Fig. 5B. As shown in the figure the intensity at the beginning of exposure is more than the one obtained at the end of earlier exposure (shown in Fig. 5A). These findings suggest a partial recovery of Pr^{3+} ions during dark storage. Such a signal recovery occurred only at temperatures exceeding 180 K. The signal recovery was also investigated by illuminating the pre-exposed samples to illumination in the wavelength range 300–450 nm. Notably, exposure to illumination with 365 nm of pre-exposed sample led to signal recovery. Fig. 5C displays the data obtained for the recovery following illumination with 365 nm for 5 min. The data was collected for the sample exposed to 275-nm illumination, shown in Fig. 5B. As seen from the figure, the intensity at the beginning of exposure (Fig. 5C) exceeds that at the end of earlier exposure shown in Fig. 5B. Additionally, the signal recovery was more than that observed to occur due to dark storage for the same time duration (Fig. 5A and B), suggesting that illumination to 365 nm leads to back-conversion to Pr^{3+} ions. The signal recovery (for pre-exposed sample) on illumination to 365 nm was noted to occur at all temperatures in the range 90–330 K, unlike the recovery associated with dark storage, which was observed only at temperatures exceeding 180 K. The samples exposed to 275-nm UV light were noted to give very weak TSL signal. These results suggest that the optical excitation dynamically changes the state of the system under observation and changes in the valence state of Pr^{3+} occur due to e/h transfer process on exposure to 275 nm f–d band, similar to those reported for $\text{ThO}_2:\text{Tb}^{3+}$ phosphor [15]. Furthermore, on dark storage and also on 365 nm illumination of the pre-exposed sample, electrons/holes are released from traps and these recombine at Pr^{4+} site resulting in the recovery of the emission signal of Pr^{3+} ions.

Salient observations from these investigations include: (I) in the entire temperature range under investigation, a fall in emission intensity of Pr^{3+} ions occurs, (II) dark storage recovery of emission

signal of pre-exposed sample occurs only at temperatures exceeding 180 K and (III) 365-nm illumination of pre-exposed sample induces signal recovery at all temperatures.

3.3. Calculation of activation energy

In photo-EPR experiments, observation of EPR signal induced either by direct photo-ionization or by capture of carriers photo-excited from other centers has been reported in the literature. The present investigations reveal that similar processes are being monitored through luminescence process, namely, $\text{Pr}^{3+} \rightarrow \text{Pr}^{4+} + e$, on 275 nm illumination and reverse process that occur partly on dark storage above 180 K and also on 365 nm illumination. Based on photo-ESR experiments of $\text{CdF}_2:\text{Eu}^{3+}$, Przybylinska and Godlewski [8] have demonstrated that activation energy for electron trapping and detrapping can be obtained by following the temperature dependence of time constants governing light-induced changes. Also the radiation induced valence changes and activation energy involved in electron release process are known to be site dependent [8,16,17].

Normally on excitation with f–d band of Pr^{3+} ions at 275 nm, a non-radiative energy transfer to low lying f^2 energy levels occurs and these low lying energy levels finally return to the ground state involving both radiative and non-radiative energy transfers. In such a process, no change in the concentration of Pr^{3+} ions is expected. While, charge transfer process can be visualized in the present case as follows. On f–d illumination of Pr^{3+} ions the excited level belonging to f^1d^1 configuration is at a lower position relative to conduction band of the host and hence there exists a small energy barrier for the electron release from Pr^{3+} ions. Owing to the existence of energy barrier, the dynamic conversion process involves activation energy and temperature dependence. Only small fraction of excited ions release the electrons to the conduction band, while, major fraction returns to ground state involving radiative and non-radiative transitions via excited states of f^2 configuration. The overall processes occurring can be represented as follows:

n_0 —number of Pr^{3+} ions in the phosphor.

$n_{\text{excited}} - n_0\alpha P$, where α is the absorption cross-section of the Pr^{3+} ions for the incident irradiation wavelength, P the density of the incident photon flux.

The excited atoms either return to ground state by non-radiative transitions via f^2 excited states and radiative/non-radiative transitions thereafter or release electrons to the conduction band. The trapping of these electrons at different trapping sites result in the reduction in the number of Pr^{3+} ions. The reduction can be represented as follows:

$$-dn/dt = n_{\text{excited}}(t)P_{\text{nr}},$$

where P_{nr} is the probability of electron transfer to conduction band $= \gamma^{-1}s e^{-E_a/kT}$ and s the frequency factor and E_a the activation energy, T the temperature, k the Boltzman constant and γ the relaxation rate of the Pr^{3+} excited state:

$$dn/dt = -n\alpha P\gamma^{-1}s e^{-E_a/kT}, \quad (1)$$

$$n(t) = n_0 e^{-(t/\tau)}, \text{ where } 1/\tau = \alpha P\gamma^{-1}s e^{-E_a/kT}.$$

The observed luminescence intensity will be proportional to $n_{\text{excited}}(t)$ reflecting the changes brought about by electron release. At a constant temperature the observed intensity can be represented as

$$I(t) = I_0 e^{-t/\tau}, \quad (2)$$

where $I(t)$ is the intensity at time t , I_0 the intensity at the beginning of exposure.

Both I_0 and $1/\tau$ will vary with temperature. The changes in $1/\tau$ will be a result of the exponential factor $e^{-E_a/kT}$ and the dependence of non-radiative transitions on temperature. For transitions between levels of a $4f^n$ configuration, the non-radiative rate is given by

$$w(T) = w(0)(n+1)^p,$$

where $W(T)$ is non-radiative rate at temperature T , $n = 1/[e^{h\nu/kT} - 1]$, p is given by $\Delta E/h\nu_{\text{max}}$ and ΔE is energy difference between the energy levels involved and ν_{max} is high vibrational frequency [18]. With the assumption that changes in non-radiative rate will not be predominantly affecting the value of $1/\tau$, in comparison to the factor $e^{-E_a/kT}$, the plot of $\ln(1/\tau)$ vs. $1/T$ will be a linear curve whose slope will be equal to $(-E_a/k)$.

In the present work, since excitation and emission intensities are monitored with a 10-nm bandwidth, the site selectivity is absent and overall intensity can be due to presence of multiple sites. The activation energy involved in the electron release process are site dependent [8,16,17] but individual sites do not influence the others and so the Eq. (2) can be modified based on the number of sites present as follows:

$$I(t) = I_{01} + I_{02}e^{-t/\tau} \quad (3)$$

(two sites with only one undergoing change),

$$I(t) = I_{01} + I_{02} \exp(-t/\tau_1) + I_{03} \exp(-t/\tau_2) \quad (4)$$

(three sites with only two undergoing change),

where I_{01} , I_{02} and I_{03} refer to intensities at the beginning of exposure for species having differences in site symmetry with three possibilities for site symmetry, i.e. sites I–III.

The data obtained at each of the temperatures were processed based on the above possibilities, using the curve fitting programs suitable for Eqs. (2–4). Fig. 6 displays typical curves obtained

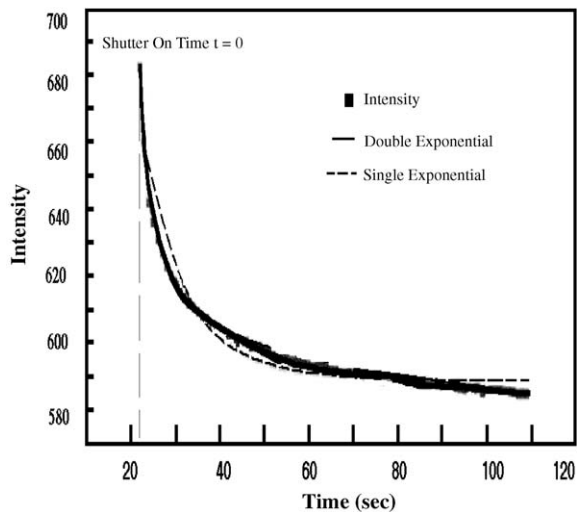


Fig. 6. Intensity variation observed with time on excitation with 275nm and monitored with 500nm emission at 180 K along with fitted curve (---) using single exponential equation $I_{01} + I_{02} \exp(-t/\tau)$ and fitted curve (—) using double exponential equation $I_{01} + I_{02} \exp(-t/\tau_1) + I_{03} \exp(-t/\tau_2)$.

for the best fit using Eqs. (3) and (4), as well as the original data obtained at 180 K. Notably, the best fit of data was obtained only when Eq. (4) involving three sites with significant value of I_{01} . Eq. (4) achieved the best fit of intensity data as a function of time at all temperatures. The time constants obtained from the best fit of data were observed to have calculated error of <5%. The spread in the values of time constants at constant temperature obtained by repetitive measurements was also found to be of the same order as that of calculated error.

Data analysis based on the type of equation required to achieve the best fit suggests the existence of Pr^{3+} ions at three different sites. Pr^{3+} ions at site I, are not involved in photoelectron transfer while those at sites II and III are involved in photoelectron transfer and have different time constants. Site dependent activation energies have been reported in the literature for laser induced bleaching of hydrogenated CaF_2 and SrF_2 crystals doped with Pr^{3+} ions [17].

The plots of $\ln(1/\tau)$ vs. $1/T$ for two sets of time constants involving two sites are shown in Figs. 7 and 8. As seen from the figures, the points can be

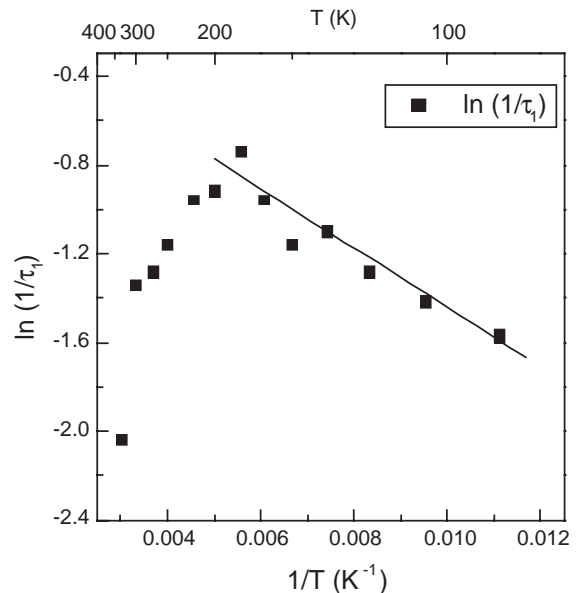


Fig. 7. Plot of $\ln(1/\tau_1)$ vs. $1/T$ along with fitted curve for 90–180 K data.

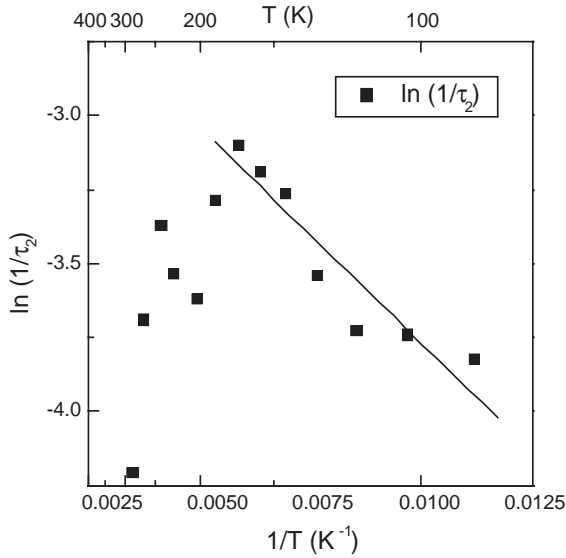


Fig. 8. Plot of $\ln(1/\tau_2)$ vs. $1/T$ along with fitted curve for 90–180 K data.

fitted with linear curve in the temperature range 90–180 K, however, beyond 180 K this trend changes. The change in trend can be possibly due to simultaneous occurrence of the electron release from Pr^{3+} ions under 275-nm f-d illumination and recapture of electrons thermally released from traps above 180 K by Pr^{4+} ions formed the earlier. As shown earlier the release of electrons from the traps and their recapture by Pr^{4+} ions leading to formation of Pr^{3+} ions leads to the observation of small signal recovery during dark storage at temperatures ≥ 180 K. In general, these observations are consistent with observations of TSL in this temperature range suggesting that some of the trap centers are unstable [10].

The simultaneous occurrence of release of electrons under photon flux by Pr^{3+} ions and the recapture by Pr^{4+} ions due to thermal stimulation above 180 K necessitates modifications in the rate equation used earlier. Since electrons are released in photo-ionization process from Pr^{3+} ions only, number of electrons, which are released and trapped, is equal to number of Pr^{4+} ions formed

$$dn/dt = -n\alpha P\gamma^{-1} s e^{-E_a/kT} r_1 + n_2 s_2 e^{-E_b/kT} r_2, \quad (5)$$

where r_1 and r_2 are the relative probabilities for a free electron to get captured by a trap and to

recombine with a Pr^{4+} ion, respectively. s_2 and E_b are frequency factor and activation energy for release of electron from trap, respectively. n_2 is the population of Pr^{4+} ions formed due to electron release from Pr^{3+} ions due to illumination. The relative probabilities can be represented by the equations:

$$r_1 = \sigma_t n_t / (\sigma_2 n_2 + \sigma_t n_t) \text{ and}$$

$$r_2 = \sigma_2 n_2 / (\sigma_2 n_2 + \sigma_t n_t),$$

where σ_2 and σ_t are the electron capture cross-sections of Pr^{4+} ions and of empty traps, and n_2 , n_t is the concentration of Pr^{4+} ions and empty traps and these populations will vary with time.

Since the population of $n_t \gg n_2$ it can be assumed that $r_1 = 1$ and $r_2 = \sigma_2 n_2 / \sigma_t n_t$ and n_t nearly constant:

$$\begin{aligned} dn/dt = & -n\alpha P\gamma^{-1} s e^{-E_a/kT} \\ & + n_2 s_2 e^{-E_b/kT} (\sigma_2 n_2 / \sigma_t n_t). \end{aligned}$$

Initially all Pr ions are present as Pr^{3+} ions only and Pr^{4+} ions are produced only as a result of illumination from the Pr^{3+} ions

$$n_0 = n \text{ (population of } \text{Pr}^{3+} \text{ ions at } t = 0) \text{ and}$$

$$n_2(t) = n_0 - n(t),$$

$$\begin{aligned} dn/dt = & -n\alpha P\gamma^{-1} s e^{-E_a/kT} + (n_0 - n) s_2 e^{-E_b/kT} \\ & \times (\sigma_2 (n_0 - n) / \sigma_t n_t), \end{aligned}$$

$$dn/dt = n^2 A_2 - n(A_1 + 2n_0 A_2) + n_0^2 A_2,$$

where

$$A_1 = \alpha P\gamma^{-1} s e^{-E_a/kT} \text{ and}$$

$$A_2 = s_2 e^{-E_b/kT} (\sigma_2 / \sigma_t n_t),$$

$$dn / (n^2 A_2 - n(A_1 + 2n_0 A_2) + n_0^2 A_2) = dt.$$

The equation is similar in form to

$$dx / (ax^2 + bx + c) \text{ where } n = x, a = A_2,$$

$$b = -(A_1 + 2n_0 A_2) \text{ and } c = n_0^2 A_2.$$

The solution of equation depends on the value of $q = 4ac - b^2$. In the present case $q = -(A_1^2 + 4n_0 A_1 A_2)$. Since A_1 , A_2 and n_0 are real and positive, $q < 0$.

The solution of the general equation is given as $1/\sqrt{(-q)} \log [(2cx + b - \sqrt{(-q)})/(2cx + b + \sqrt{(-q)})]$.

In the present case, the above equations with proper substitution will be equal to $(t + \text{constant})$.

The solution will not have the simple exponential time dependence and the exact solutions cannot lead to the Eq. (4) arising from multiplicity of sites. The values of $\ln(1/\tau)$ obtained by the curve fitting obtained with Eq. (4) in the temperature range where both processes are occurring simultaneously cannot be proper and hence lead to the deviation in the plots τ shown in Figs. 7 and 8, at temperatures above 180 K.

Hence, the activation energy involved in the release of electron during 275-nm exposure can be determined only from the slopes of the curves obtained in the linear range of 90–180 K. The slopes for the two centers were found to be 131 ± 20 and 139 ± 40 , respectively. Nearly the same values of slope, having a magnitude of difference smaller than the calculated error, lead to almost same activation energy for the two sites viz. 12 ± 3.5 meV.

4. Conclusion

In conclusion, investigations of the charge transfer processes in $\text{ThO}_2:\text{Pr}^{3+}$ phosphor have revealed that Pr^{3+} ions probably occupy three different sites, two of which undergo charge transfer on illumination with f–d band at 275 nm with the activation energy ≈ 12 meV for the two sites. Moreover, the mobility of the electrons

released from traps and their recapture at Pr^{4+} ion sites is responsible for the deviation from linearity in the plot of $\ln(\tau)$ vs. $(1/T)$ above 180 K.

References

- [1] B. Henderson, G.F. Imbush, *Optical Spectroscopy of Inorganic Solids*, Clarendon Press, Oxford, 1989.
- [2] C. Pedrini, D.S. McClure, C.H. Anderson, *J. Chem. Phys.* 70 (1979) 4959.
- [3] W.C. Wong, D.S. McClure, S.A. Basun, M.R. Kokta, *Phys. Rev. B* 51 (1995) 5682.
- [4] S.A. Basun, T. Danger, A.A. Kaplyanskii, D.S. McClure, K. Petermann, W.C. Wong, *Phys. Rev. B* 54 (1996) 6141.
- [5] I.A. de Carcer, G. Lifante, F. Cusso, F. Jaque, T. Calderon, *Appl. Phys. Lett.* 58 (1991) 1825.
- [6] J. Fleniken, J. Wang, J. Grimm, M.J. Weber, U. Happek, *J. Lumin.* 94–95 (2001) 465.
- [7] A. Hofstaetter, M.V. Korzhik, V.V. Laguta, B.K. Meyer, V. Nagirnyi, R. Novotny, *Radiat. Meas.* 33 (2001) 533.
- [8] H. Przybylinska, M. Godlewski, *Solid State Commun.* 50 (1984) 425.
- [9] M. Bryesse, L. Faure, H. Pralraud, *Chem. Phys. Lett.* 61 (1979) 132.
- [10] P.J. Harvey, J.B. Hallett, *J. Lumin.* 14 (1976) 131.
- [11] O.K. Moune, M.D. Faucher, N. Edelstein, *J. Lumin.* 96 (2002) 51.
- [12] E.T. Rodin, P.L. Land, *Phys. Rev. B* 4 (1971) 2701.
- [13] H.E. Hoefdradd, G. Blasse, *Phys. Stat. Sol. A* 29 (1974) K95.
- [14] S.V. Godbole, J.S. Nagpal, A.G. Page, *Radiat. Meas.* 32 (2000) 343.
- [15] S.V. Godbole, J.S. Nagpal, A.G. Page, *Radiat. Meas.* 32 (2000) 349.
- [16] R.J. Reeves, G.D. Jones, R.W.G. Syme, *Phys. Rev. B* 40 (1989) 6475.
- [17] K.M. Murdoch, G.D. Jones, *Phys. Rev. B* 58 (1998) 12020.
- [18] G. Blasse, B.C. Grabmair, *Luminescent Materials*, Springer, Berlin, 1994, p. 74.